High probability of transitions in the H-I spectrum and 3D-atomic orbitals geometry

Diana R. RADNEF-CONSTANTIN*,[1], Sorin S. RADNEF[2], Liliana PREDA[3], Mark RUSHTON[1], Agneta A. MOCANU[4], Dan PRICOPI[1], Valentin I. NICULESCU[5]

*Corresponding author
[1]Department of Astrophysics and Cosmology,
Astronomical Institute of the Romanian Academy,
Strada Cuțitul de Argint 5, Bucharest, Romania,
ghe12constantin@yahoo.com
[2]Department of Systems,
INCAS – National Institute for Aerospace Research "Elie Carafoli",
B-dul Iuliu Maniu 220, Bucharest, Romania
[3]National University of Science and Technology POLITEHNICA Bucharest,
Splaiul Independentei 313, 060042, Bucharest, Romania
[4]Department of Physics, Hyperion University,
Calea Calarasilor 169, Sector 3, Bucharest, 030615,Romania
[5]National Institute for Laser, Plasma and Radiation Physics,
Strada Atomistilor 409, Magurele, Ilfov, 077125, Romania

DOI: 10.13111/2066-8201.2026.18.1.7

Received: 12 February 2026/ Accepted: 23 February 2026/ Published: March 2026

Abstract: *In the framework of the quantum model for hydrogen atom, we use the wave functions provided by the solutions of the Schrödinger equation with Coulomb potential. Considering the radial and angular densities of the localization probability, we identify the representative quantum states that play a high-probability role in transitions for H-I spectra. Besides that, we obtain some other complementary results. So, we present the numerical tables for the radial distributions, the electron density functions and some observables like θ nodal angles, nodal surfaces, along with the ordered sequences of the average radii in the sub-shells associated with this n:* $\langle r\rangle_{4f} = 18a_0 < \langle r\rangle_{4d} = 21a_0 < \langle r\rangle_{4p} = 23a_0 < \langle r\rangle_{4s} = 24a_0$ *(a_0 - the first Bohr radius). Further, we have added the significant scientific 3D-visualization of the orbitals shapes and describe them via the nodal values for θ angles.*

Key Words: *spectroscopy, astrophysics, quantum geometry, hydrogen, probability of transition, representative quantum state, 3D atomic orbitals visualization*

1. INTRODUCTION

The of Schrödinger's work [1], [2] and others paved the way for development of Quantum Mechanics, Spectroscopy and QED. On the one hand, there are various and important theoretical aspects [3], some of which refer to the search for analytical solutions of the Schrödinger's equation with different potentials [4]-[6]. On the other hand, historically

speaking, there are several atomic models: the planetary model: the planetary model, the Bohr's model [7] and those models with fine [8] and hyperfine structure. These models are the basis for understanding atomic-scale processes and phenomena in various plasma types.
Several topics of interest - for Quantum and Atomic Physics [9] and their applications in Astrochemistry and Astrophysics [10] include: a) the spectrum of light from various cosmic sources, such as galaxies, stars and interstellar clouds [11]-[13] as well as b) [14]. Since atomic orbitals are essential for understanding the structure of atoms, molecules, gases, and plasma [15], [16] and in order to identify certain representative quantum states regarding the highest probability of transition, we are developing a method of theoretical spectroscopy which we exemplify by analyzing the hydrogen orbitals in the excited states with $n = 2, 3, 4$. The structure of our paper is as follows: In section 2, we describe the mathematical framework of the hydrogen-like atom (H-like atom) [17] with a fine structure which consists of key equations or functions as quantum entities, such as wave eigen functions and observables. In section 3, we tabulate our derived values of maximum localization density, and those of electron density depending on an angular factor, finding some representative states, and we obtain the following observables: average radii, nodal angles θ and nodal surfaces. We also construct 3D geometric representations of orbital shapes generated by spherical harmonics corresponding to quantum states with n up to 4.
Finally, we give a synthesis, consisting of three sets of results: 1) an analysis to identity the representative quantum states, 2) the value data of a few observables such as θ nodal angles, nodal surfaces, and some order relations for the average-radii of sub-shells, and 3) an atomic orbitals scientific 3D-visualization, where all of these are exemplified for shells with n less than 5.

2. METHOD: BASIC QUANTUM FORMULAE AND ENTITIES

For the 3D modelling of the atomic orbitals, we relied on several key equations and concepts of quantum physics as follows: The general form of Schrödinger's equation is [9]:

$$i\hbar\frac{\partial\Psi}{\partial t} = \hat{H}\Psi = \left(-\frac{\hbar^2}{2\mu}\nabla^2 + V\right)\Psi \tag{1}$$

For a non-temporal potential $V=V(r)$ with spherical symmetry [5], [18] the Schrödinger's equation becomes (the so called the stationary case or independent time equation):

$$\left[\frac{-\hbar^2}{2\mu}\nabla^2 + V(r)\right]\Psi_{n\ell m}(r,\theta,\phi) = E_n\Psi_{n\ell m}(r,\theta,\phi) \tag{2}$$

It is well known the general form of wave function:

$$\overline{\Psi}_{n\ell m}(r,\theta,\varphi,t) = \Psi_{n\ell m}(r,\theta,\varphi)e^{\frac{-i}{\hbar}E_n t} \tag{3}$$

where for the Coulomb-potential the space components are:

$$\Psi_{n\ell m}(r,\theta,\varphi) = \Re_{n\ell}(r)Y_\ell^m(\theta,\varphi) \tag{4}$$

where the radial components formula is:

$$\Re_{n\ell}(r) = -\sqrt{\left(\frac{2}{na_\mu}\right)^3\frac{(n-\ell-1)}{2n[(n+\ell)!]^3}}e^{\frac{-r}{na_\mu}}\left(\frac{2r}{na_\mu}\right)^\ell L_{n+\ell}^{2\ell+1}\left(\frac{2r}{na_\mu}\right) \tag{5}$$

with the associated, respectively general, Laguerre's polynomials and m being the electron mass, reduce mass μ and a_0-the first Bohr radius.

$$a_\mu = \frac{m}{\mu} a_0 \qquad L_j^k(x) = (-1)^k \frac{d^k}{dx^k} L_{j+k}(x) \qquad L_j(x) = e^x \frac{d^j}{dx^j} e^{-x} x^j \tag{6}$$

The angular components have the following formulae:

$$Y_\ell^m(\theta, \varphi) = (-1)^m \sqrt{\frac{(2\ell+1)(\ell-m)!}{4\pi(\ell+m)!}} P_\ell^m(\cos\theta) e^{im\varphi} \qquad m \geq 0 \tag{7}$$

and

$$Y_\ell^{\odot m}(\theta, \varphi) = (-1)^{|m|} Y_\ell^{|m|}(\theta, \varphi) \qquad m < 0 \tag{8}$$

where the associated, respectively general, Legendre's polynomials are:

$$P_\ell^m(x) = (-1)^m \sqrt{(1-x^2)^m} \frac{d^m}{dx^m} P_\ell(x) \qquad for\ m \geq 0 \tag{9}$$

$$P_\ell(x) = \frac{(-1)^\ell}{2^\ell \ell!} \frac{d^\ell}{dx^\ell} (1-x^2)^\ell \tag{10}$$

For a quantum state described by the numbers ($n\ \ell\ m$), we compute the probability density of electron localization using the formula:

$$|\Psi_{n\ell m}(r, \theta, \phi)|^2 \tag{11}$$

The average radius formula of the state ($n\ \ell\ m$) is:

$$\langle r \rangle_{n\ell} = \frac{n^2 a_\mu}{Z} \left[1 + \frac{1}{2} \left(1 - \frac{\ell(\ell+1)}{n^2} \right) \right] \tag{12}$$

We mention that in our analysis we need to define some useful quantum entities as follows: $DML_{n\ell}(r) = (r\ \Re_{n\ell}(r))^2$ - the radial distribution function and $Del_{\ell m}(w) = |Y_\ell^m(\theta, \varphi)|^2$ - the electron density in angular factor function, where $w=cos(\theta)$.
These functions are important tools for our method of theoretical spectroscopy to identify the representative quantum states.
We will develop this method in the RESULTS section. Also, considering the formulae of angular components (9-10) and in order to simplify our presentation, we make the convention $m=|m|$.

3. RESULTS

The α, β, γ *Ly* lines denoted in the H-emission spectra [18] correspond to the transitions from the levels $n \in \{2,3,4\}$ to the ground state [19], [20]. We develop a computational program, and use mathematical software to analyses and represent in three spatial dimensions the quantum states associated with these fixed n.

3.1 Representative quantum states

To find the representative quantum states, we will proceed to develop a method that will help us in this aspect.

The physical significance of the probability density function $|\Psi_{n\ell m}(\theta,\varphi)|^2$ allows us to identify situations in which these functions reach maxima.
Taking into account the convention $m=|m|$ in which we work, we start with case $n=2$ and we obtain the below results. The radial distribution $DML_{2\ell}$ reaches its maximum value for $\ell=1$ as seen in the Table 1

Table 1: Numerical values of $DML_{2\ell}$

ℓ	$DML_{2\ell}$ (r)	$\langle r\rangle_{2\ell}$ [a_0]
0	$DML_{20}(5.23) = 0.190$	$\langle r\rangle_{2s} = 6$
1	$DML_{21}(4.00) = 0.195$	$\langle r\rangle_{2p} = 5$

Also, for the average radii $\langle r\rangle_{2\ell}$ corresponding to the shell with $n=2$, we obtain the order relation:

$$5a_0 = \langle r\rangle_{2p} < \langle r\rangle_{2s} = 6a_0 \tag{13}$$

The electron density in the angular factor $Del_{\ell m}$ reaches its maximum value for $m=0$ as seen in the Table 2:

Table 2: Numerical values of $Del_{\ell m}$

m	$Del_{1m}(w)$
0	$Del_{10}(1) = 0.238$
1	$Del_{11}(0) = 0.119$

So, for shell $n=2$, the probability function reaches its maximum on the orbital $\ell=1$ and $m=0$. We conclude that the quantum state (*2 1 0*) is a representative quantum state [21]. The quantum case $n=3$ is analyzed in the same manner as the previous one. In the table we see that the radial distribution $DML_{3\ell}$ reaches its maximum value for $\ell=2$.

Table 3: Numerical values of $DML_{3\ell}$

ℓ	$DML_{3\ell}$ (r)	$\langle r\rangle_{3\ell}$ [a_0]
0	$DML_{30}(13.07) = 0.1015$	$\langle r\rangle_{3s} = 13.5$
1	$DML_{31}(`12.00) = 0.1017$	$\langle r\rangle_{3p} = 12.5$
2	$DML_{32}(9.00) = 0.1070$	$\langle r\rangle_{3d} = 10.5$

Also, for the average radii $\langle r\rangle_{3\ell}$ we obtain the sub-shells order relation:

$$\langle r\rangle_{3d} = 10.5\ a_0 < \langle r\rangle_{3p} = 12.5\ a_0 < \langle r\rangle_{3s} = 13.5\ a_0 \tag{14}$$

In the table we see that the electron density in the angular factor Del_{2m} reaches its maximum value for $m=0$.

Table 4: Numerical values of Del_{2m}

m	$Del_{2m}(w)$
0	$Del_{20}(1.000) = 0.397$
1	$Del_{21}(0.707) = 0.149$
2	$Del_{22}(0.000) = 0.149$

So, for the shell n=3 the probability function reaches its maximum on the sub-shell ℓ=2 and the orbital with m=0. The state (*3 2 0*) is also a representative state. Finally, for the quantum case n=4 we obtain the following: In Table 5, we see that the radial distribution $DML_{4\ell}$ reaches its maximum value for ℓ=3.

Table 5: Numerical values of $DML_{4\,\ell}$

ℓ	$DML_{4\ell}(r)$	$\langle r\rangle_{4\ell}$ [a_0]
0	$DML_{40}(24.60) = 0.06440$	$\langle r\rangle_{4s} = 24$
1	$DML_{41}(23.60) = 0.06444$	$\langle r\rangle_{4p} = 23$
2	$DML_{42}(21.21) = 0.0649$	$\langle r\rangle_{4d} = 21$
3	$DML_{43}(16.00) = 0.0697$	$\langle r\rangle_{4f} = 18$

For average radii $\langle r \rangle_{4\ell}$ we obtain the sub-shells order relation:

$$\langle r\rangle_{4f} = 18a_0 < \langle r\rangle_{4d} = 21a_0 < \langle r\rangle_{4p} = 23a_0 < \langle r\rangle_{4s} = 24a_0 \quad (15)$$

In Table 6, we see that the electron density in the angular factor Del_{3m} reaches also its maximum value for m=0.

Table 6: Numerical values of Del_{3m}

m	$Del_{3m}(w)$
0	$Del_{30}(1.00) = 0.557$
1	$Del_{31}(0.86) = 0.198$
2	$Del_{32}(0.58) = 0.154$
3	$Del_{33}(0.00) = 0.174$

Considering our findings in the analysis for the above cases, we derive that the state (*4 3 0*) is a representative quantum state, too.

3.2 The 3D-representation of the representative quantum states

For the states *(n ℓ m)* - after the computation of electron localization probability density.
The average radius formula of the state (n ℓ m) is:

$$|\Psi_{n\ell m}(r,\theta,\varphi)|^2$$

in the spherical coordinates system with colatitude $\theta \in (0, \pi)$ and azimuth $\varphi \in [0, 2\pi]$ we build the 3D geometric representations [22] and we explain the shape of orbitals which correspond to those quantum states.

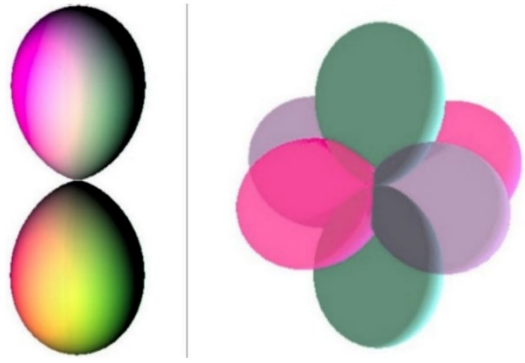

Figure 1: The 3D representation of $2p_z$ – orbital (left) and $2p_x$, $2p_y$, $2p_z$ – superposed orbitals (right)

We remark that for all representative quantum states - identified by us in the above sub-section - the orbital magnetic quantum number is m=0, and as we can easily observe in eq. (9), the harmonic functions Y_ℓ^m always take real values. Starting with Figure 1, we describe the representative quantum states. The mathematical expression for the spherical harmonic [23] corresponding to the state (*2 1 0*) is:

$$Y_1^0(\theta, \varphi) = \sqrt{\frac{3}{4\pi}} cos(\theta) \tag{16}$$

For this state, we find θ nodal value $\theta_{nod} = 90^o$ and, taking into account the rotation around the azimuth φ, we obtain a nodal surface (namely the plan at $\theta = 90^o$).
The derived shape of $3d_z$ – orbital which has the following spherical harmonic formula:

$$Y_2^0(\theta, \varphi) = \sqrt{\frac{15}{4\pi}} (3cos^2(\theta) - 1) \tag{17}$$

For this state we find as nodal values $\theta_{nod} \in \{55^o, 125^o\}$. Taking into account the rotation about the azimuth φ we obtain the corresponding nodal surfaces (the conic surfaces at $\theta \in \{55^o, 125^o\}$, these cones orientated upwards and downwards, respectively).

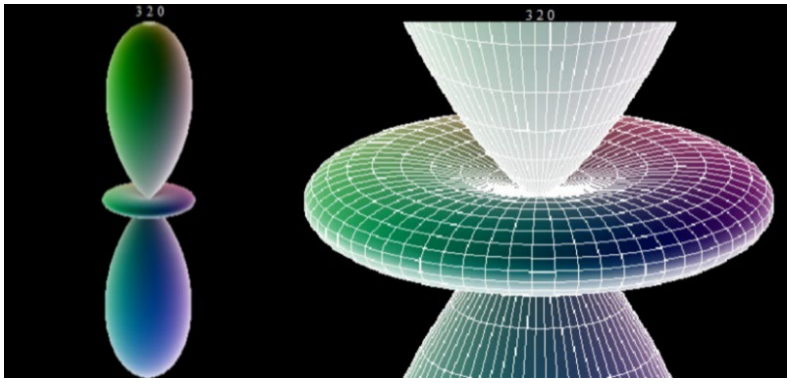

Figure 2: The 3D representation of $3d_z$ – orbital shown as whole (left) and zoomed to bring out the detail (right)

Continuing our analysis, the spherical harmonic for the quantum state (*4 3 0*) is:

$$Y_3^0(\theta,\varphi) = \sqrt{\frac{7}{4\pi}}(5cos^3(\theta) - cos(\theta)) \tag{18}$$

Considering this formula we find the corresponding nodal values $\theta_{nod} \in \{39^o, 90^o, 141^o\}$ and, taking into account the rotation about the azimuth φ, we also obtain the corresponding nodal surfaces (the plan at $\theta = 90^o$ and two conic surfaces at $\theta \in \{39^o, 141^o\}$, these ones orientated upwards and downwards, respectively).

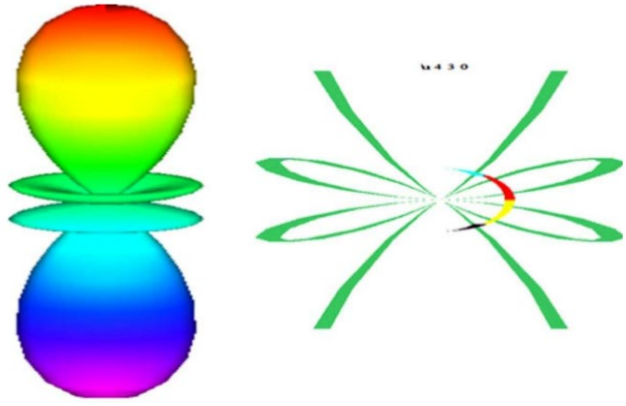

Figure 3: The 3D representation of $4f_z$ – orbital (left) and its longitudinal section with the multicolored arc added over the section (right).

In the right-panel of Figure 3, we illustrate these nodal values by dividing in longitude the $4f_z$ - state longitudinally (see the sequential colored arc that follows the nodal values θ and the arc added over this longitudinal-section).

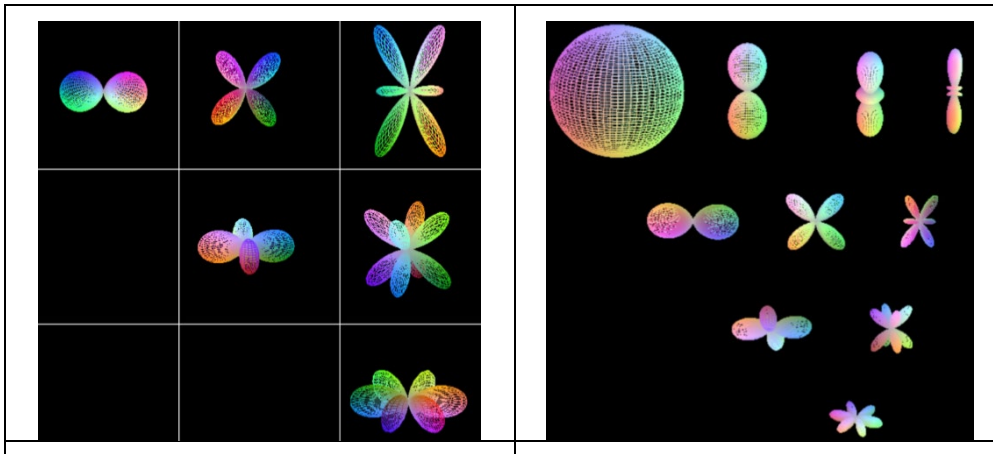

panel a) panel b)

Figure 4: panel a) the 3D orbital shapes of states (from the upper left to lower right): (*4 1 1*), (*4 2 1*), (*4 3 1*), (*4 2 2*), (*4 3 2*), (*4 3 3*), obtained by using the real part of harmonic components; panel b) the 3D atomic orbitals of hydrogen with $n \leq 4$.

Additively, in Figure 4 (in both panels), we build the 3D shape visualization of the orbitals for the rest of states with n=4, namely those with non-zero m [24].

4. CONCLUSIONS AND DISCUSSIONS

In our approach, we have developed a method of theoretical spectroscopy which has helped us to find the representative quantum states; these states can be related to the ones with the highest probability of transition [19], [21], [25].
We have developed a graphical representation for the 3D shapes of these orbitals, emphasizing the role of nodal angles θ in the generation of the nodal surfaces; thus, we explain the orbital configuration. Furthermore, we have obtained a relation between the average radii in the sub-shells associated with $n \leq 4$, such as:

$$\langle r \rangle_{4f} = 18a_0 < \langle r \rangle_{4d} = 21a_0 < \langle r \rangle_{4p} = 23a_0 < \langle r \rangle_{4s} = 24a_0 \quad (19)$$

Thus, for the hydrogen orbitals in the excited states with $n \leq 4$, we found as representative quantum states (*2 1 0*), (*3 2 0*), (*4 3 0*), and constructed a 3D visualization of them and for the states with non-zero m. Consequently, we propose that representative states (*2 1 0*), (*3 2 0*), (*4 3 0*) are most likely the quantum states defining the transitions for the α, β, γ Lyman hydrogen emission lines, respectively. The representation of orbitals leads to a better assessment of the spatial distributions for these states, and this is useful in assessing the temperatures both of plasma and its electrons [16], [26]. Note that these orbitals are suitable for studying several atoms (alkali metals) and ionic species X^+, namely the hydrogen-like atoms. Considering the results of the preceding analysis and the useful intuitive meaning of the 3D graphical representations, these subjects for a deeper insight into the quantum world will be continued.

ACKNOWLEDGEMENTS

In memory of Prof. Dr. Constantin Udriste from the Politehnica University of Bucharest. We also thank dr. Bonciocat Anca from Simion Stoilow Institute of Mathematics, Bucharest and dr. Erika Varga-Verebelyi from Konkoly Observatory, Budapest, for valuable advice and support for our work.

REFERENCES

[1] E. Schroedinger, *Quantisierung als Eigenwertproblem (zweite Mitteilung)*, Wann.der Physik, **79**, 489 – 527, 1926.
[2. W. A. Fedak, J. J. Prentis, The 1925 Born and Jordan paper On quantum mechanics, *Am. J. Phys.* **77**, 128, 2009.
[3] O. Olkhov, Geometrical Approach in Atomic Physics: Atoms of Hydrogen and Helium, **Am. J. Phys. 2**, 108 – 112, 2014.
[4] C. Berkdemir, Application of the Nikiforov-Uvarov Method in Quantum Mechanics, *Theoretical Concepts of Quantum Mechanics*, InTech, 226 – 251, 2012.
[5] D. R. Constantin, V. I. Niculescu, *Treatment of the quasi-harmonic potential with the centrifugal type term in the Schrödinger equation via Laplace transform*, 2018, https://arxiv.org/abs/1804.02455
[6] V. D. Wytse, Analytic time-dependent solutions of the one-dimensional Schroedinger equation, *Am. J. Phys.* **82**, 955, 2014.
[7] K. Helge, Niels Bohr and the Quantum Atom: The Bohr Model of Atomic Structure 1913 – 1925, *Am. J. Phys.* **81**, 237, 2013.
[8] C. Keebaugh, E. Marshman, Ch. Singh, Improving student understanding of fine structure corrections to the energy spectrum of the hydrogen atom, *Am. J. Phys.* **87**, 594, 2019.
[9] B. H. Bransden, Ch. Joachain, *Physics of Atoms and Molecules,* 2003.
[10] I. N. Levine, *Quantum Chemistry,* 7th ed.; Pearson, 2014.
[11] Z. Zheng, J. Wallace, *Anisotropic Lyman-Alpha emission from Star-forming Galaxies*, IAU General Assembly, 2015.
[12] S. A. Brown, L. Fletcher, G. S. Kerr, N. Labrosse, A. F. Kowalski, J. De La Cruz Rodríguez, Modeling of the Hydrogen Lyman Lines in Solar Flares, *The Astrophysical Journal* **862**, 59, 2018.

[13] K. K. Nilsson, *Thesis: The Lyα Emission Line asa Cosmological Tool*, Kobenhavns Universitet, Danmark, https://arxiv.org/abs/0711.2199v1, 2007.
[14] M. Montgomery, *Stellar Oscillations: Pulsations of stars throughout the H-R diagram*, https://www.as.utexas.edu/ mikemon/pulsations.pdf, 2013.
[15] I. Mayer, Effective atomic orbitals: A tool for understanding electronic structure of molecules*, Int. J. Quant. Chem.* **114**, 1041-1047, 2014, https://onlinelibrary.wiley.com/doi/full/10.1002/qua.24623
[16] N. Vanhaecke, D. Comparat, D. A. Tate, P. Pillet, Ionization of Rydberg atoms embedded in an ultra-cold plasma, *Phys. Rev.A*, **71**, 2005.
[17] D. R. Constantin, V. I. Niculescu, A. A. Mocanu, D. Pricopi, E. Verebelyi-Varga, The orbitals of Rydberg atom, *Rom. Astron. J.*, **30**, 1, 2020.
[18] W. A. Fedak, J. J. Prentis, Quantum jumps and classical harmonics, *Am. J. Phys*. **70**, 332, 2002.
[19] D. R. Radnef-Constantin et al., *The Quantum Spectral Model for all α– multiplets and the spectral composition în the fine structure of Humphreys α– line of H-I, 2024, , https://papers.ssrn.com/sol3/papers.cfm?abstract_id=4744616* (preprint)
[20] D. Constantin, L. Preda, A. A. Mocanu, D. Popescu, D. Pricopi, V. I. Niculescu, The quantum states for Hydrogen atom: spherical harmonics and the orbitals geometrical representation, *INCAS BULLETIN*, Volume **16**, Issue 1, https://doi.org/10.13111/2066-8201.2024.16.1.2, 2024.
[21] D. R. Constantin, L. Preda, M. Rushton, Hydrogen-like atoms and spectra: special quantum states and maximum relative intensity line of its multiplet, *U.P.B. Sci. Bull., Series A*, Vol. **1**, pp. 167-176, 2023.
[22] D. R. Radnef-Constantin and S. S. Radnef, Intrinsic Curvatures of Atomic Orbitals for Hydrogen-Like Atoms, *INCAS BULLETIN*, Volume **17**, Issue 1, pp. 61 – 68, https://doi.org/10.13111/2066-8201.2025.17.1.6, 2025,
[23] D. R. Constantin et al., Hydrogen-like atoms and spectra: orbitals scientific 3D-visualization and states with the highest probability of transition, *Quant.Chem* 2022 (preprint)
[24] D. R. Constantin, V. I. R. Niculescu, A. A. Mocanu, F. Nacu, E. Verebelyi-Varga, *The Hydrogen-like atom: geometric representation of its orbital types*, BSG Proceedings 27. pp. 17-21, Balkan Society of Geometers, Geometry Balkan Press 2020.
[25] J. Tennyson, S. Miller, *Hydrogen molecular ions: H_3^+ H_5^+ and beyond*, *Philosophical Transactions of The Royal Society A Mathematical Physical and Engineering Sciences*, 2019.
[26] J. Tatum, *Stellar Atmosphere*, 2003, http://orca.phys.uvic.ca/ tatum/intro.html